DAFTAR PUSTAKA

[1] K. C. Vinoth Kumar *et al.*, "Spectral characterization of hydroxyapatite extracted from Black Sumatra and Fighting cock bone samples: A comparative analysis," *Saudi J Biol Sci*, vol. 28, no. 1, pp. 840–846, Jan. 2021, doi: 10.1016/j.sjbs.2020.11.020.

[2] Y. Wibisono *et al.*, "Marine-derived biowaste conversion into bioceramic membrane materials: Contrasting of hydroxyapatite synthesis methods," *Molecules*, vol. 26, no. 21, Nov. 2021, doi: 10.3390/molecules26216344.

[3] L. Zhang, H. Liu, H. Yao, Y. Zeng, and J. Chen, "Preparation, Microstructure, and Properties of ZrO2(3Y)/Al2O3 Bioceramics for 3D Printing of All-ceramic Dental Implants by Vat Photopolymerization," *Chinese Journal of Mechanical Engineering: Additive Manufacturing Frontiers*, vol. 1, no. 2, p. 100023, Jun. 2022, doi: 10.1016/j.cjmeam.2022.100023.

[4] A. Sabir, H. Abbas, A. Y. Amini, and S. Asmal, "Characterization of duck egg shells and bioceramic materials in making denture applications," *IOP Conf Ser Mater Sci Eng*, vol. 1088, no. 1, p. 012116, Feb. 2021, doi: 10.1088/1757-899x/1088/1/012116.

[5] M. Das *et al.*, "3D printing of tough nature inspired hierarchical architecture using chicken bone and eggshell biowaste for biomedical applications," *Ceram Int*, vol. 49, no. 17, pp. 29274–29287, Sep. 2023, doi: 10.1016/j.ceramint.2023.06.220.

[6] H. Hamidah, Iriany, and M. Zuqni, "Characterization of hydroxyapatite from chicken bone via precipitation," in *Key Engineering Materials*, Trans Tech Publications Ltd, 2017, pp. 485–489. doi: 10.4028/www.scientific.net/KEM.744.485.

[7] B. Nayak and P. K. Misra, "Exploration of the structural and dielectric characteristics of a potent hydroxyapatite coated gallium bioceramics for the forthcoming biomedical and orthopedic applications," *Mater Chem Phys*, vol. 239, Jan. 2020, doi: 10.1016/j.matchemphys.2019.121967.

[8] N. D. Malau and F. Adinugraha, "Synthesis of hydrokxyapatite based duck egg shells using precipitation method," in *Journal of Physics: Conference Series*, IOP Publishing Ltd, Jun. 2020. doi: 10.1088/1742-6596/1563/1/012020.

[9] S. Tlili, S. Bouyegh, K. Labiod, N. Traiaia, and M. Hassani, "Synthesis and characterization of hydroxyapatite powder derived of eggshell by precipitation method."

[10] N. Tangboriboon and J. Suttiprapar, “Innovative Preparation Calcium Hydroxyapatite from Duck Eggshell via Pyrolysis,” *Applied Mechanics and Materials*, vol. 851, pp. 8–13, Aug. 2016, doi: 10.4028/www.scientific.net/amm.851.8.

[11] B. Musa, I. Raya, and H. Natsir, “Synthesis and Characterizations of Hydroxyapatite Derived Blood Clam Shells (Anadara granosa) and Its Potency to Dental Remineralizations,” 2016. [Online]. Available: http://www.ripublication.com

[12] M. Khoirudin and dan Zultiniar Laboratorium Teknik Reaksi Kimia, “SINTESIS DAN KARAKTERISASI HIDROKSIAPATIT (HAp) DARI KULIT KERANG DARAH (Anadara granosa) DENGAN PROSES HIDROTERMAL,” 2015.

[13] K. V, M. R, and A. P, “Sol-Gel Mediated Synthesis of Pure Hydroxyapatite at Different Temperatures and Silver Substituted Hydroxyapatite for Biomedical Applications,” *J Biotechnol Biomater*, vol. 07, no. 04, 2017, doi: 10.4172/2155-952x.1000275.

[14] S. Edi Cahyaningrum, F. Afifah, and J. Angelo Ranamanggala, “INDONESIAN CHEMISTRY AND APPLICATION JOURNAL PEMANFAATAN LIMBAH TULANG IKAN MANYUNG (Arius thalassinus) SEBAGAI MATERIAL IMPLAN GIGI,” vol. 4, no. 2, doi: 10.26740/icaj.v4n2.p21-26.

[15] N. Ismiati and D. Darwis, “The effect of sintering temperature on the mechanical properties of ceramic,” in *Journal of Physics: Conference Series*, IOP Publishing Ltd, Feb. 2021. doi: 10.1088/1742-6596/1763/1/012094.

[16] D. O. Obada, E. T. Dauda, J. K. Abifarin, D. Dodoo-Arhin, and N. D. Bansod, “Mechanical properties of natural hydroxyapatite using low cold compaction pressure: Effect of sintering temperature,” *Mater Chem Phys*, vol. 239, Jan. 2020, doi: 10.1016/j.matchemphys.2019.122099.

[17] M. Megha *et al.*, “Structural and biological properties of novel Vanadium and Strontium co-doped HAp for tissue engineering applications,” *Ceram Int*, vol. 49, no. 18, pp. 30156–30169, Sep. 2023, doi: 10.1016/j.ceramint.2023.06.272.

[18] R. Liu, L. Ma, H. Liu, B. Xu, C. Feng, and R. He, “Effects of pore size on the mechanical and biological properties of stereolithographic 3D printed HAp bioceramic scaffold,” *Ceram Int*, vol. 47, no. 20, pp. 28924–28931, Oct. 2021, doi: 10.1016/j.ceramint.2021.07.053.

[19] M. Sari, P. Hening, Chotimah, I. D. Ana, and Y. Yusuf, “Bioceramic hydroxyapatite-based scaffold with a porous structure using honeycomb as a

natural polymeric Porogen for bone tissue engineering," *Biomater Res*, vol. 25, no. 1, Dec. 2021, doi: 10.1186/s40824-021-00203-z.

[20] L. S. Taji, D. E. Wiyono, A. Dwitama Karisma, A. Surono, and E. O. Ningrum, "Hydroxyapatite Based Material: Natural Resources, Synthesis Methods, 3D Print Filament Fabrication, and Filament Filler."

[21] V. Rodríguez-Lugo *et al.*, "Wet chemical synthesis of nanocrystalline hydroxyapatite flakes: Effect of pH and sintering temperature on structural and morphological properties," *R Soc Open Sci*, vol. 5, no. 8, Aug. 2018, doi: 10.1098/rsos.180962.

[22] A. Nur Ismawati, A. Iryani, and L. J. Kusumawardani, "EFFECTIVENESS HYDROXYAPATITE FROM CHICKEN EGGSHELLS FOR ADSORPTION OF CHROMIUM (VI) METAL ION ELECTROPLATING WASTE," *Helium: Journal of Science and Applied Chemistry*, vol. xx, [Online]. Available: https://journal.unpak.ac.id/index.php/he_jsac

[23] R. Foroutan, S. J. Peighambardoust, S. S. Hosseini, A. Akbari, and B. Ramavandi, "Hydroxyapatite biomaterial production from chicken (femur and beak) and fishbone waste through a chemical less method for Cd2+ removal from shipbuilding wastewater," *J Hazard Mater*, vol. 413, Jul. 2021, doi: 10.1016/j.jhazmat.2021.125428.

[24] S.-L. Bee, M. Mariatti, N. Ahmad, B. H. Yahaya, and Z. A. A. Hamid, "Effect of the calcination temperature on the properties of natural hydroxyapatite derived from chicken bone wastes," 2019. [Online]. Available: www.sciencedirect.comwww.materialstoday.com/proceedings2214-7853

[25] E. Barua, A. B. Deoghare, P. Deb, S. Das Lala, and S. Chatterjee, "Effect of Pre-treatment and Calcination Process on Micro-Structural and Physico-Chemical Properties of Hydroxyapatite derived from Chicken Bone Bio-waste," 2019. [Online]. Available: www.sciencedirect.comwww.materialstoday.com/proceedings2214-7853

[26] P. Temperatur Sintering dan Komposisi Air dalam Suspensi terhadap Ukuran Kristal Hidroksiapatit Berbasis Tulang Sapi Aceh, I. Salsabila, dan Zulkarnain Jalil Jurusan Fisika, F. Matematika dan Ilmu PengetahuanAlam, and U. Jl Syekh Abdul Rauf, "The Effect of Sintering Temperature and Water Composition in Suspension to the Crystallite Size of Hydroxyapatite Based on Aceh's Bovine Bone," *J. Aceh Phys. Soc*, vol. 7, no. 3, pp. 157–161, 2018, [Online]. Available: http://www.jurnal.unsyiah.ac.id/JAcPS

[27] A. R. Gintu, E. B. E. Kristiani, and Y. Martono, "Hydroxiapatite (HAp) Bioceramics Made from The Caletaiya presclupta Snail Shells from Poso

Lake," *JKPK (Jurnal Kimia dan Pendidikan Kimia)*, vol. 5, no. 3, p. 254, Dec. 2020, doi: 10.20961/jkpk.v5i3.45983.

[28] M. W. Teoh *et al.*, "Synthesis and Characterization of Chicken Bone-Derived Hydroxyapatite Incorporating Pectin," *Chem Eng Technol*, Dec. 2023, doi: 10.1002/ceat.202300019.

[29] Supriyono *et al.*, "The Formation Process of Hydroxyapatite Nanoparticles by Electrolysis and Their Physical Characteristics," *International Journal of Technology*, vol. 14, no. 2, pp. 330–338, 2023, doi: 10.14716/ijtech.v14i2.4452.

[30] Charlena, A. Maddu, and T. Hidayat, "Synthesis and Characterization of Hydroxyapatite from Green Mussel Shell with Sol-Gel Method," *Jurnal Kimia Valensi*, vol. 8, no. 2, pp. 269–279, Nov. 2022, doi: 10.15408/jkv.v8i2.27494.

[31] J. K. Abifarin, "Taguchi grey relational analysis on the mechanical properties of natural hydroxyapatite: effect of sintering parameters," *International Journal of Advanced Manufacturing Technology*, vol. 117, no. 1–2, pp. 49–57, Nov. 2021, doi: 10.1007/s00170-021-07288-9.

[32] A. Gupta, T. Vennila, K. Andiyappan, S. Shreepad, M. Sathiyamoorthy, and A. S. A. L. G. Gopala Gupta, "Characterization of the hydroxyapathite obtained from chicken egg shell applied in bioceramics," *Mater Today Proc*, Sep. 2023, doi: 10.1016/j.matpr.2023.09.079.

[33] S. El-Gebaly, N. El-Faramawy, and H. Kahil, "Thermoluminescence response of bone hydroxyapatite," *Opt Mater (Amst)*, vol. 134, Dec. 2022, doi: 10.1016/j.optmat.2022.113089.

[34] O. A. Osuchukwu, A. Salihi, I. Abdullahi, P. O. Etinosa, and D. O. Obada, "A comparative study of the mechanical properties of sol-gel derived hydroxyapatite produced from a novel mixture of two natural biowastes for biomedical applications," *Mater Chem Phys*, vol. 297, Mar. 2023, doi: 10.1016/j.matchemphys.2023.127434.

[35] M. Mathina, E. Shinyjoy, L. Kavitha, P. Manoravi, and D. Gopi, "A comparative study of naturally and synthetically derived bioceramics for biomedical applications," in *Materials Today: Proceedings*, Elsevier Ltd, 2019, pp. 3600–3603. doi: 10.1016/j.matpr.2019.08.222.

[36] M. Baladi *et al.*, "Green sol–gel synthesis of hydroxyapatite nanoparticles using lemon extract as capping agent and investigation of its anticancer activity against human cancer cell lines (T98, and SHSY5)," *Arabian Journal of Chemistry*, vol. 16, no. 4, Apr. 2023, doi: 10.1016/j.arabjc.2023.104646.

[37] S. Türk, İ. Altınsoy, G. Çelebi Efe, M. Ipek, M. Özacar, and C. Bindal, "Effect of Solution and Calcination Time on Sol-gel Synthesis of Hydroxyapatite," *J Bionic Eng*, vol. 16, no. 2, pp. 311–318, Mar. 2019, doi: 10.1007/s42235-019-0026-3.

[38] M. S. Islam, A. M. Z. Rahman, M. H. Sharif, A. Khan, M. Abdulla-Al-Mamun, and M. Todo, "Effects of compressive ratio and sintering temperature on mechanical properties of biocompatible collagen/hydroxyapatite composite scaffolds fabricated for bone tissue engineering," *Journal of Asian Ceramic Societies*, vol. 7, no. 2, pp. 183–198, Apr. 2019, doi: 10.1080/21870764.2019.1600226.

[39] B. De Carvalho *et al.*, "Effect of sintering on in vivo biological performance of chemically deproteinized bovine hydroxyapatite," *Materials*, vol. 12, no. 23, Dec. 2019, doi: 10.3390/ma12233946.

[40] A. Fitriadi Akbar *et al.*, "SINTESIS DAN KARAKTERISASI HIDROKSIAPATIT TULANG IKAN BAUNG (Hemibagrus nemurus sp.) SEBAGAI KANDIDAT IMPLAN TULANG," 2021.

[41] N. Rani, S. Chahal, A. S. Chauhan, P. Kumar, R. Shukla, and S. K. Singh, "X-ray Analysis of MgO Nanoparticles by Modified Scherer's Williamson-Hall and Size-Strain Method," 2019. [Online]. Available: www.sciencedirect.comwww.materialstoday.com/proceedings

[42] H. Khandelwal and S. Prakash, "Synthesis and Characterization of Hydroxyapatite Powder by Eggshell," *Journal of Minerals and Materials Characterization and Engineering*, vol. 04, no. 02, pp. 119–126, 2016, doi: 10.4236/jmmce.2016.42011.

[43] S. Kurapati #1 and K. Srivastava, "APPLICATION OF DEBYE-SCHERRER FORMULA IN THE DETERMINATION OF SILVER NANO PARTICLES SHAPE."

[44] A. B. D. Nandiyanto, R. Oktiani, and R. Ragadhita, "How to read and interpret ftir spectroscope of organic material," *Indonesian Journal of Science and Technology*, vol. 4, no. 1, pp. 97–118, 2019, doi: 10.17509/ijost.v4i1.15806.

[45] Charlena, I. H. Suparto, and D. P. O. Laia, "Synthesis and Characterization of Hydroxyapatite from Polymesoda placans Shell using Wet Precipitation Method," *J Bios Logos*, vol. 13, no. 1, pp. 85–96, Feb. 2023, doi: 10.35799/jbl.v13i1.47454.

[46] N. Selvia, K. Dahlan, and S. U. Dewi, "SINTESIS DAN KARAKTERISASI β-TRICALCIUM PHOSPHATE BERBASIS CANGKANG KERANG RANGA PADA VARIASI SUHU SINTERING," 2012.

[47] A. O. Bokuniaeva and A. S. Vorokh, “Estimation of particle size using the Debye equation and the Scherrer formula for polyphasic TiO2 powder,” in *Journal of Physics: Conference Series*, Institute of Physics Publishing, Dec. 2019. doi: 10.1088/1742-6596/1410/1/012057.

[48] M. A. Siddiqui, F. Hussain, A. A. Mohamad, S. Hanif, and M. Tufail, “Effect of Calcination and Sintering Temperatures on Physical Properties of Barium Titanate Ceramic.” [Online]. Available: https://www.researchgate.net/publication/330113226

[49] V. Kulyk *et al.*, “The Effect of Sintering Temperature on the Phase Composition, Microstructure, and Mechanical Properties of Yttria-Stabilized Zirconia,” *Materials*, vol. 15, no. 8, Apr. 2022, doi: 10.3390/ma15082707.

[50] M. Trzaskowska, V. Vivcharenko, and A. Przekora, “The Impact of Hydroxyapatite Sintering Temperature on Its Microstructural, Mechanical, and Biological Properties,” *International Journal of Molecular Sciences*, vol. 24, no. 6. Multidisciplinary Digital Publishing Institute (MDPI), Mar. 01, 2023. doi: 10.3390/ijms24065083.

[51] P. Temperatur Sintering dan Komposisi Air dalam Suspensi terhadap Ukuran Kristal Hidroksiapatit Berbasis Tulang Sapi Aceh, I. Salsabila, dan Zulkarnain Jalil Jurusan Fisika, F. Matematika dan Ilmu PengetahuanAlam, and U. Jl Syekh Abdul Rauf, “The Effect of Sintering Temperature and Water Composition in Suspension to the Crystallite Size of Hydroxyapatite Based on Aceh’s Bovine Bone,” *J. Aceh Phys. Soc*, vol. 7, no. 3, pp. 157–161, 2018, [Online]. Available: http://www.jurnal.unsyiah.ac.id/JAcPS

[52] J. K. Odusote, Y. Danyuo, A. D. Baruwa, and A. A. Azeez, “Synthesis and characterization of hydroxyapatite from bovine bone for production of dental implants,” *J Appl Biomater Funct Mater*, vol. 17, no. 2, Apr. 2019, doi: 10.1177/2280800019836829.

[53] P. Cangkang *et al.*, “Sintesis Biomaterial Hidroksiapatit Porous dengan.”

[54] S. Campbell and K. M. Poduska, “Incorporating far-infrared data into carbonate mineral analyses,” *Minerals*, vol. 10, no. 7, pp. 1–11, Jul. 2020, doi: 10.3390/min10070628.

[55] M. Sahadat Hossain and S. Ahmed, “FTIR spectrum analysis to predict the crystalline and amorphous phases of hydroxyapatite: a comparison of vibrational motion to reflection,” *RSC Adv*, vol. 13, no. 21, pp. 14625–14630, May 2023, doi: 10.1039/d3ra02580b.

[56] J. K. Abifarin, D. O. Obada, E. T. Dauda, and D. Dodoo-Arhin, “Experimental data on the characterization of hydroxyapatite synthesized

from biowastes," *Data Brief*, vol. 26, Oct. 2019, doi: 10.1016/j.dib.2019.104485.

[57] M. Jurusan *et al.*, "Sintesis dan Karakterisasi Hidroksiapatit dari Cangkang Kerang Darah dengan Proses Hidrotermal Variasi Suhu dan pH Bona Tua 1) , Amun Amri 2) , dan Zultiniar 2) 1)," 2016.

[58] A. M. Kurniawan, S. Hartini, and M. N. Cahyanti, "Eksakta: Jurnal Ilmu-ilmu MIPA The effect of Phosphate Concentration on Ca/P Ratio of Hydroxyapatite from Ceramic Industrial Gipsum Waste Pengaruh Konsentrasi Fosfat Terhadap Perbandingan Ca/P Hidroksiapatit dari Limbah Gipsum Industri Keramik," vol. 19, no. 1, pp. 46–56, 2019.

[59] M. Fazhlur Arrafiqie, Y. Azis, D. Zultiniar, M. Jurusan, T. Kimia, and D. Jurusan, "Sintesis Hidroksiapatit dari Limbah Kulit Kerang Lokan (Geloina expansa) Dengan Metode Hidrothermal," 2016.

[60] H. Gheisari, E. Karamian, and M. Abdellahi, "A novel hydroxyapatite - Hardystonite nanocomposite ceramic," *Ceram Int*, vol. 41, no. 4, pp. 5967–5975, May 2015, doi: 10.1016/j.ceramint.2015.01.033.

[61] S. Chadijah, "ANALISIS HIDROKSIAPATIT DARI TULANG IKAN TUNA (THUNNUS ALBACORES) DENGAN XRF, FTIR, dan XRD," *Al-Kimia*, vol. 6, no. 2, Dec. 2018, doi: 10.24252/al-kimia.v6i2.5067.

[62] A. M. Kurniawan, S. Hartini, and M. N. Cahyanti, "Eksakta: Jurnal Ilmu-ilmu MIPA The effect of Phosphate Concentration on Ca/P Ratio of Hydroxyapatite from Ceramic Industrial Gipsum Waste Pengaruh Konsentrasi Fosfat Terhadap Perbandingan Ca/P Hidroksiapatit dari Limbah Gipsum Industri Keramik," vol. 19, no. 1, pp. 46–56, 2019.

LAMPIRAN

Lampiran 1. Dokumentasi Penelitian

Tulang ayam direbus selama 1 jam

Tulang ayam direndam dalam aseton selama 2 jam

Tulang ayam dibersihkan dengan menggunakan pisau

Tulang ayam dikeringkan di bawah sinar matahari

Tulang ayam dihaluskan dengan blender

Tulang ayam dihaluskan dengan alu dan mortar

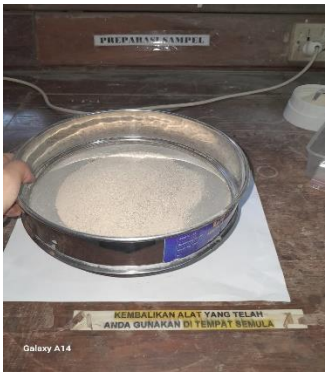

Tulang ayam diayak

Kalsinasi tulang ayam

CaO

Etanol

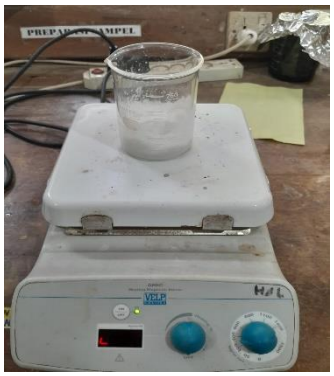

Stirrer CaO + Etanol

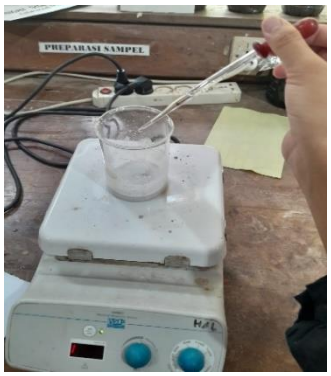

Proses penambahan asam posfat

Proses Pengecekan pH

Proses pemanasan

Proses Pengendapan selama 24 jam

Sampel dioven

Sampel disintering pada suhu 700℃, 800℃ dan 900℃

HAp pada suhu sintering 700℃

HAp pada suhu sintering 800℃

HAp pada suhu sintering 900℃

HAp tanpa sintering

Lampiran 2 Analisis Data

2.1 Analisis Data *X-Ray Diffraction* (XRD)

Tabel 1. Analisis data XRD untuk ukuran kristal HAp tanpa sintering

Sudut Difraksi (2θ)	θ	Cos θ	B FWHM (rad)	Ukuran Kristal
25,86	12,93	0,974644167	0,1914	41,77184679
28,98	14,49	0,968191325	0,2758	29,03635615
31,86	15,93	0,961597733	0,2064	38,86470403
32,94	16,47	0,958968314	0,2199	36,50321347
34,04	17,02	0,956202641	0,1762	45,58870006
39,76	19,88	0,940406885	0,2032	39,69172065
46,78	23,39	0,917823927	0,2007	40,42204623
49,48	24,74	0,90821623	0,2111	38,52724966
Rata-rata			0,210588	38,80072963

Tabel 2. Analisis data XRD untuk ukuran kristal HAp pada suhu sintering 700℃

Sudut Difraksi (2θ)	θ	Cos θ	B FWHM (rad)	Ukuran Kristal
26,56	13,28	0,973259116	0,2080	38,45161979
27,56	13,78	0,971217485	0,2206	36,27415077
28,79	14,395	0,96860486	0,1200	66,7282155
29,52	14,76	0,967001488	0,2207	36,29655073
32,12	16,06	0,960972522	0,2189	36,65122693
35,07	17,535	0,953533082	0,2207	36,42145697
46,43	23,215	0,919032174	0,1700	47,70676673
Rata-rata			0,196986	42,64714106

Tabel 3. Analisis data XRD untuk ukuran kristal HAp pada suhu sintering 800℃

Sudut Difraksi (2θ)	θ	Cos θ	B FWHM (rad)	Ukuran Kristal
26,54	13,27	0,973299193	0,18	44,43253165
27,56	13,78	0,971217485	0,2533	31,36316231
28,79	14,395	0,96860486	0,2328	34,39598737
29,44	14,72	0,967179116	0,224	35,76021015
32,12	16,06	0,960972522	0,2473	32,44218995
35,07	17,535	0,953533082	0,21	38,27721692
46,31	23,155	0,919444457	0,12	67,57732747
Rata-rata			0,209629	40,60694655

Tabel 4. Analisis data XRD untuk ukuran kristal HAp pada suhu sintering 900℃

Sudut Difraksi (2θ)	θ	Cos θ	B FWHM (rad)	Ukuran Kristal
27,67	13,835	0,970988387	0,2457	32,57038139
29,46	14,73	0,967134753	0,2066	38,77239786
30,5	15,25	0,964787324	0,2	40,07580583
32,24	16,12	0,960682295	0,256	31,34198182
34,4	17,2	0,955278362	0,233	34,48337897
39,88	19,94	0,940050268	0,1866	43,22668211
Rata-rata			0,221317	36,74510466

Lampiran 3 Data *Fourier Transform Infrared* (FTIR)

Data *Fourier Transform Infrared* **(**FTIR) Tanpa Sintering

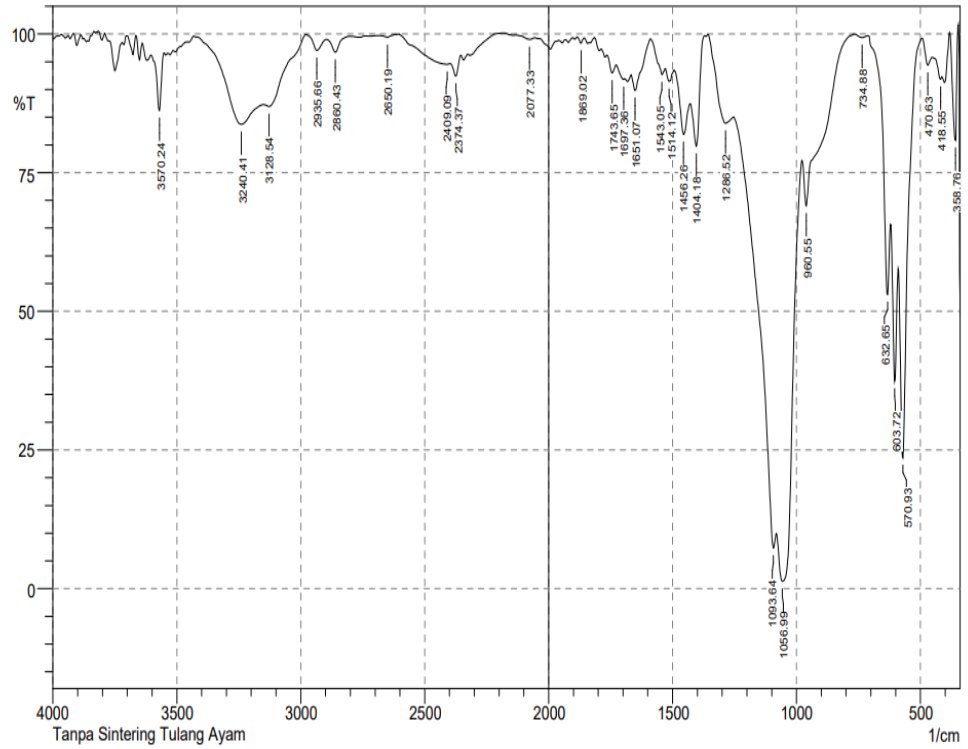

No.	Peak	Intensity	Corr. Intensity	Base (H)	Base (L)	Area	Corr. Area
1	358.76	80.856	20.118	381.91	349.12	1.516	1.629
2	418.55	91.858	0.756	451.34	414.7	0.984	0.038
3	470.63	94.389	2.961	493.78	451.34	0.728	0.26
4	570.93	23.619	41.37	588.29	493.78	18.357	8.338
5	603.72	37.421	23.947	619.15	590.22	9.127	2.966
6	632.65	53.022	17.272	705.95	621.08	7.936	1.797
7	734.88	99.362	0.457	765.74	711.73	0.098	0.061
8	960.55	69.012	9.741	975.98	767.67	13.606	2.803
9	1056.99	1.33	23.816	1080.14	977.91	92.63	38.666
10	1093.64	7.308	7.77	1251.8	1082.07	63.315	2.421
11	1286.52	83.896	5.865	1355.96	1253.73	5.361	1.655

Data *Fourier Transform Infrared* **(**FTIR) Sintering 700℃

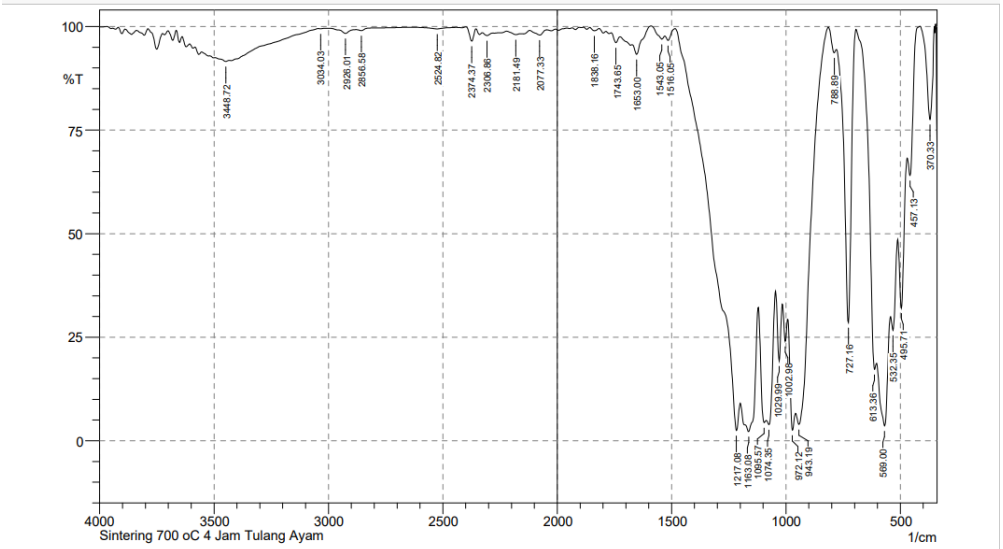

	Peak	Intensity	Corr. Intensity	Base (H)	Base (L)	Area	Corr. Area
1	370.33	77.58	21.888	412.77	352.97	2.932	2.834
2	457.13	64.072	10.952	468.7	414.7	4.417	0.935
3	495.71	32.077	24.008	511.14	470.63	13.739	4.183
4	532.35	26.686	9.396	542	513.07	13.792	1.854
5	569	3.623	21.627	603.72	543.93	59.278	22.074
6	613.36	17.254	8.528	692.44	605.65	20.723	0.96
7	727.16	28.568	68.866	779.24	694.37	15.615	14.457
8	788.89	93.692	2.263	813.96	779.24	0.625	0.184
9	943.19	3.951	11.561	956.69	815.89	64.427	6.623
10	972.12	2.601	13.336	991.41	958.62	37.112	8.48
11	1002.98	24.001	6.955	1014.56	993.34	12.054	1.234

Data *Fourier Transform Infrared* **(**FTIR) Sintering 800℃

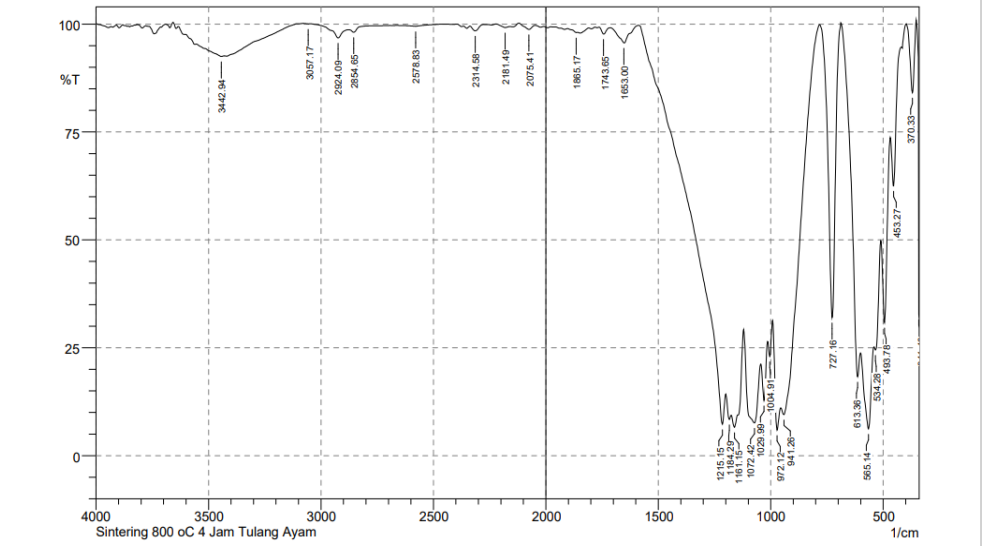

No.	Peak	Intensity	Corr. Intensity	Base (H)	Base (L)	Area	Corr. Area
1	341.4	31.937	30.189	343.33	339.47	1.891	0.424
2	370.33	84.111	16.49	397.34	352.97	1.452	1.552
3	453.27	62.522	17.077	466.77	420.48	4.965	1.59
4	493.78	30.811	27.972	509.21	468.7	13.448	4.779
5	534.28	24.498	5.62	540.07	511.14	14.113	1.408
6	565.14	6.192	18.442	599.86	542	50.701	15.363
7	613.36	18.287	15.897	686.66	601.79	24.827	3.022
8	727.16	31.998	68.119	781.17	688.59	14.467	14.499
9	941.26	9.511	8.531	954.76	783.1	66.844	3.376
10	972.12	5.917	14.15	991.41	956.69	32.756	6.982
11	1004.91	23.001	5.284	1012.63	993.34	11.355	0.959

Data *Fourier Transform Infrared* **(**FTIR) Sintering 900℃

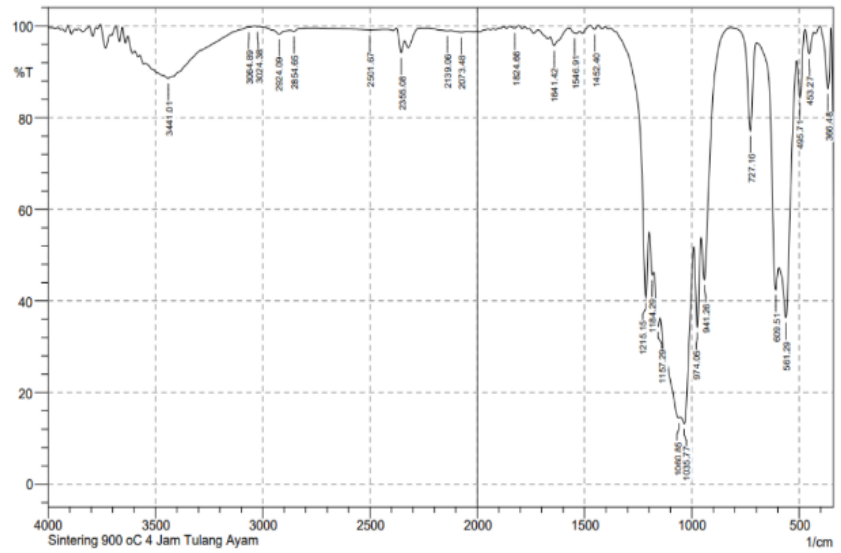

No.	Peak	Intensity	Corr. Intensity	Base (H)	Base (L)	Area	Corr. Area
1	366.48	86.311	13.287	403.12	352.97	1.465	1.403
2	453.27	93.979	4.985	472.56	432.05	0.627	0.442
3	495.71	84.32	10.915	511.14	474.49	1.61	0.943
4	561.29	36.391	29.13	594.08	513.07	21.424	7.174
5	609.51	42.459	11.222	698.23	596	13.001	1.334
6	727.16	77.128	19.958	817.82	700.16	3.454	2.478
7	941.26	44.636	14.166	956.69	819.75	13.87	1.939
8	974.05	34.247	18.224	991.41	958.62	12.177	2.992
9	1035.77	13.211	11.206	1051.2	993.34	36.609	4.672
10	1060.85	14.458	1.909	1147.65	1053.13	62.69	2.032
11	1157.29	34.385	4.633	1176.58	1149.57	11.383	0.787